



Methods for the Determination of the Heat Transfer Coefficient in Air Cooled Condenser Used at Biomass Power Plants

Yanán Camaraza-Medina

Technical Sciences Faculty, Universidad de Matanzas, Matanzas 44440, Cuba

Corresponding Author Email: yanan.camaraza@umcc.cu

<https://doi.org/10.18280/ijht.390505>

ABSTRACT

Received: 9 October 2019

Accepted: 11 October 2020

Keywords:

flow condensation, heat transfer coefficient, mathematical deduction

In the present work, its show a summary of functional relationships developed for the application of dry condensation systems to Biomass Power Plants that present difficulties with access to water for condensation. The bibliographic review reveals the limitations of the analyzed works, in terms of the development of mathematical models and empirical correlations that allow evaluating the simultaneous effects of the surrounding meteorological variables on the average coefficient of heat transfer and the effect on the environment of the use of dry condensation. The analytical study is based on the weak solutions and their correlation with experimental quantities available in research already established in the area of action, a procedure is developed for the calculation of the average coefficients of heat transfer that includes the influence of local climatologically variables, the effect of the spatial distribution of the tubes package on the refrigerant and the confined confinement in inclined components, which increase the reliability of the thermo-hydraulic analysis and suppresses the need for the use of excess areas required by current methods. The proposed models and correlations allow the preparation of a procedure, by means of which all the possible operative variants are evaluated.

1. INTRODUCTION

At the end of 2019, about 32 percent of water withdrawals for industrial purposes were used in wet condensers. In areas with limited access to water, the most widespread solution is the use of dry condensers, which achieve savings rates of water consumption close to 95 percent [1, 2].

The Cuban state has planned an investment that will allow the installation of 1650 MW of power, (solar, wind and biomass), which represents 24 percent of the national energy matrix. Of these, 875 MW correspond to 25 Biomass Power Plant (BPP) projects, which require high volumes of water for their condensation system, however, these requirements violate Law 124/2017 on the use of terrestrial waters [3].

Given the downturn of the water deficit and the potentiality of the use of biomass as an energy source, the use of ACC can be an effective solution, however in its evaluation there are inconveniences [4].

ACC uses air as refrigerant, which is why, the installation evidences a low global heat transfer coefficient, besides than the variation of the environmental temperature and the velocity of the wind affect this heat transfer coefficient perceptibly. The vapor condenses in the inside of inclined tubes, however, at the present time, does not count on a procedure that it enables getting from reliable way, the values of the heat transfer coefficients for this type of configuration [5-7].

The methods currently used in the evaluation of the global coefficient K in an ACC are imprecise, because they do not include the effect of local climatic variables, the influence of the geometry of the tube package on the refrigerant and the condensation confined in inclined components, so the use of

excess area is required in the operation of these facilities [8-13].

For this reason, the main objective of the present work is to define a procedure for the calculation of the average heat transfer coefficients that includes the influence of local climatic variables, the effect of the spatial distribution of the tube package on the refrigerant and the condensation confined in inclined components, which increases the reliability of thermo-hydraulic analysis and eliminates the need to use excess areas required by current methods.

2. EXTERNAL FLOW

2.1 External heat transfer coefficient α_L

An analysis of 783 experimental data sets reported in eight specialized papers on the subject, allowed to develop a dimensionally non-homogeneous expression, which was generated by an integral analysis of residues by cross-jump methods at intervals (Breshnetzov method), which correlates with an average error of $\pm 6.9\%$ in 84.8% percent of the available experimental samples. This equation is given by the following expression [14]:

$$\alpha_L = \frac{(1 + \log_{10}(T_{TBS}/V_V)^{0.015}) \cdot (V_m)^{0.06} (e_a \cdot h_a)^{0.01}}{(0.15 \cdot (S_T - d_e)^{0.4}) \cdot \ln(F)^{0.28}} \quad (1)$$

where: S_T is the transverse step, in m; V_V is the velocity of the incident wind on the ACC installation, in m/s; V_m is the velocity in the narrowest section of the tube package, in m/s;

e_a is the fins thickness, in mm; d_e is the outer diameter of the bare tubes (without fins), in m; h_a is the height of the fins, in mm; F is the number of fins per linear meter of finned tube length; T_{TBS} is dry bulb temperature, in °C. Value of V_m is determined by using the following criteria [15]:

$$\begin{aligned} \text{if } 2(S_D - d_E) > (S_T - D) &\rightarrow V_m = \frac{S_T}{S_T - d_E} V_0 \\ \text{if } 2(S_D - d_E) \leq (S_T - D) &\rightarrow V_m = \frac{S_T}{2(S_D - d_E)} V_0 \end{aligned} \quad (2)$$

where: V_0 is the rate of entry of the cooling agent into the tube package, in m/s; S_T is the transverse step, in m; S_L is the longitudinal step, in m; D is the outer diameter of the tubes + fins, which make up the package, in m; S_D is the diagonal step, in m,

Table 1 gives the validity parameters of Eq. (1), while all the experimental data used in its development and validation are given by Camaraza-Medina et al. [14].

Table 1. Validity range of the Eq. (1)

Parameter	Range	Parameter	Range
Tube inclination ACC	45-60°	h_a (mm)	2.5-7.9
d_e (mm)	19-50	V_0 (m/s)	0.1-100
S_T/S_L	0.4-2	T_{TBS} (°C)	15-43
V_v (m/s)	0-45	e_a (mm)	1.3-3.5

The deviation is determined by the following expression:

$$E = 100 \cdot \left| \frac{\alpha_L - \alpha_{exp}}{\alpha_L} \right| \quad (3)$$

In Eq. (3) α_{exp} is the average experimental heat transfer coefficient, while the mean absolute error (MAE) is determined as:

$$MAE = \frac{1}{N} \sum_N \left| \frac{\alpha_L - \alpha_{exp}}{\alpha_L} \right| \quad (4)$$

In Eq. (4), N is the amount of experimental data available. In Tables 2 and 3 the validity range of the Eq. (1) is fragmented in six zones, the average and maximum deviation obtained in

its correlation with the available experimental data being given in each case.

In Figures 1 and 2, the values of MAE and E_{max} obtained in the correlation developed between available experimental data and selected models are given in graphical form [15].

The study shows that in the first and second range, the fundamentals results used in the comparison concentrate on two fundamental elements, described early (MAE and E_{max}). In these, it is confirmed that the model given by Camaraza et al. (Eq. (3)) [14] have the best MAE adjustment values, showing an average error of 7.6% and 7.2% in the correlation with available experimental data for zones 1 and 6, respectively.

In the specialized literature it is established that Zukauskas's model correlates with an average error of 25%; however, the results obtained in the present study show an average error of 29.6% and 32.3% in the correlation with available experimental data for zones 1 and 6, respectively, proving that the values obtained in the present study are slightly higher to the values commonly attributed in the literature.

The most unfavorable indicators are obtained using the models of Griminson and *Engineering Sciences Data Unit* (ESDU), which provide MAE values of 33.2% and 29.1% respectively for zone 1, while the MAE values of 28.2% and 27.4% respectively for zone 6. The models of Gray-Webb, Briggs-Young and Rabas-Eckels allows to obtain convenient results, with MAE values of 15.3% to 27.1%, which agrees well with those results given by Camaraza [15].

The specialized literature does not count with reports that suggest the possible maximum executed error with the use of a determined model. In the present study the value of E_{max} generated with the use of every model for the six studied zones was obtained, by means of the correlation made between the experimental available data and the models selected.

The model developed by Camaraza et al. [14] shows the best E_{max} index, with 11.5% and 12.9% respectively in Zone 1, and 6. On the contrary, the most unfavorable indicators are obtained with the correlations of Griminson and Zukauskas, which provide E_{max} values of 41.4% and 38.5% respectively for Zone 1, increasing to 48.2% and 43.1% in Zone 6. The other models analyzed in this study provide fairly acceptable adjustments of correlation. The early elements allows affirming that the proposed model (Eq. (3)) constitutes a scientific novelty.

Table 2. Correlation of the first range of values with Eq. (1)

Valid for $0.4 \leq S_T/S_L \leq 1$; $19 \leq d_e \leq 50$ mm and $1.3 \leq e_a \leq 3.5$ mm					
Zone	Validity range	Deviation	Zone	Validity range	Deviation
1	$2.5 \leq h_a \leq 4.7$	MAE < 7.6% for 89.9% of the data	2	$2.5 \leq h_a \leq 5.1$	MAE < 6.8% for 88.1% of the data
	$0 \leq V_v \leq 5.4$			$0 \leq V_v \leq 10.1$	
	$0 \leq V_0 \leq 10$	E_{max} < 11.5% $N=79$		$0 \leq V_0 \leq 28.2$	E_{max} < 9.3% $N=135$
	$15 \leq T_{TBS} \leq 18$			$15 \leq T_{TBS} \leq 24$	
3	$115 \leq F \leq 194$	MAE < 5.9% for 87.3% of the data	4	$115 \leq F \leq 254$	MAE < 6.1% for 88.4% of the data
	$2.5 \leq h_a \leq 5.1$			$2.5 \leq h_a \leq 6.4$	
	$0 \leq V_v \leq 16.2$			$0 \leq V_v \leq 24.1$	
	$0 \leq V_0 \leq 41.4$			$0 \leq V_0 \leq 65.6$	
5	$15 \leq T_{TBS} \leq 30$	E_{max} < 11.2% $N=192$	6	$15 \leq T_{TBS} \leq 35$	E_{max} < 12.1% $N=232$
	$115 \leq F \leq 315$			$115 \leq F \leq 354$	
	$2.5 \leq h_a \leq 7.9$	MAE < 6.2% for 89.7% of the data		$2.5 \leq h_a \leq 7.9$	MAE < 7.5% for 90.5% of the data
	$0 \leq V_v \leq 38.2$			$0 \leq V_v \leq 45$	
5	$0 \leq V_0 \leq 88.4$	E_{max} < 12.6% $N=282$	6	$0 \leq V_0 \leq 100$	E_{max} < 12.9% $N=368$
	$15 \leq T_{TBS} \leq 40$			$15 \leq T_{TBS} \leq 43$	
	$115 \leq F \leq 354$			$115 \leq F \leq 394$	

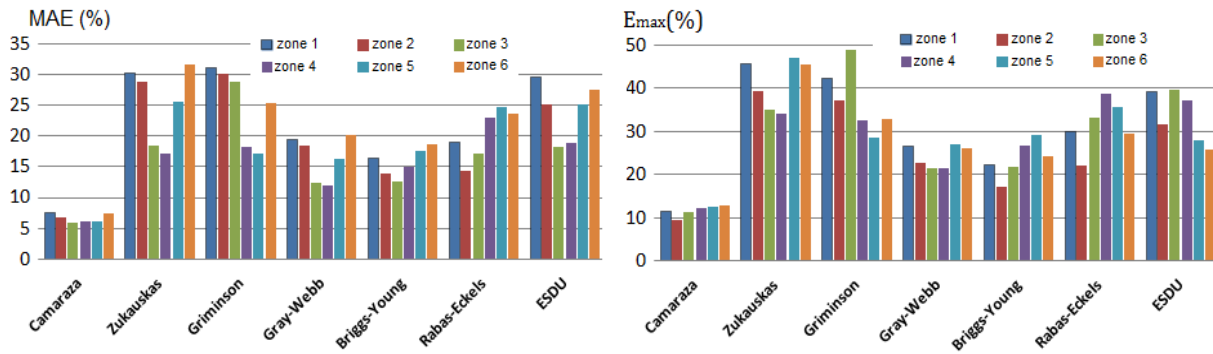


Figure 1. MAE and E_{max} values obtained in the correlation data with other models for $(0.4 \leq S_T/S_L \leq 1)$

Table 3. Correlation of the second range of values with Eq. (1)

Valid for $1 < S_T/S_L \leq 2$; $19 \leq d_e \leq 50$ mm and $1.3 \leq e_a \leq 3.5$ mm					
Zone	Validity range	Deviation	Zone	Validity range	Deviation
1	$2.5 \leq h_a \leq 4.7$	MAE < 6.5% for	2	$2.5 \leq h_a \leq 5.1$	MAE < 7.1% for
	$0 \leq V_i \leq 5.4$	89.4% of the data		$0 \leq V_i \leq 10.1$	88.3% of the data
	$0 \leq V_o \leq 10$	$E_{max} < 11.8\%$		$0 \leq V_o \leq 28.2$	$E_{max} < 10.9\%$
	$15 \leq T_{TBS} \leq 18$	$N=82$		$15 \leq T_{TBS} \leq 24$	$N=146$
3	$115 \leq F \leq 194$	MAE < 7.3% for	4	$115 \leq F \leq 254$	MAE < 6.0% for
	$2.5 \leq h_a \leq 5.1$	87.6% of the data		$2.5 \leq h_a \leq 6.4$	90.1% of the data
	$0 \leq V_i \leq 16.2$	$E_{max} < 9.5\%$		$0 \leq V_i \leq 24.1$	$E_{max} < 10.9\%$
	$0 \leq V_o \leq 41.4$	$N=207$		$0 \leq V_o \leq 65.6$	$N=302$
5	$15 \leq T_{TBS} \leq 30$	MAE < 6.2% for	6	$15 \leq T_{TBS} \leq 35$	MAE < 6.4% for
	$115 \leq F \leq 315$	89.9% of the data		$115 \leq F \leq 354$	90.6% of the data
	$2.5 \leq h_a \leq 7.9$	$E_{max} < 11.3\%$		$2.5 \leq h_a \leq 7.9$	$E_{max} < 11.8\%$
	$0 \leq V_i \leq 38.2$	$N=356$		$0 \leq V_i \leq 45$	$N=15$
	$0 \leq V_o \leq 88.4$				
	$15 \leq T_{TBS} \leq 40$				
	$115 \leq F \leq 354$				

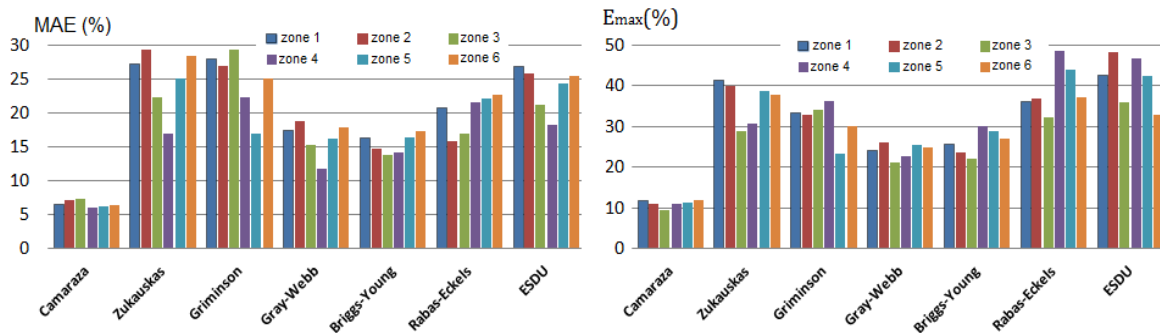


Figure 2. MAE and E_{max} values obtained in the correlation data with other models for $(1 < S_T/S_L \leq 2)$

3. INTERNAL FLOW

3.1 Heat transfer coefficient α_T

The combination of the differential equations of the velocity profile and temperature distribution, and their subsequent homogenization by means of gamma functions, allowed to obtain a theoretical solution for the determination of the α_T coefficient inside vertical tubes. The developed expression is given by Medina et al. [16]:

$$Nu_{vert} = 0.943 \cdot \sqrt[4]{d_i^3 \frac{\sin \varphi \cdot g \cdot (\rho_L - \rho_V) \cdot r_{LV}}{\nu_L \cdot \lambda_L \cdot (T_{sat} - T_P)}} \quad (5)$$

where: d_i is the equivalent inner tube diameter, in m; g is the

gravitational acceleration, in m/s^2 ; ρ_L is the liquid density, in kg/m^3 ; ρ_V is the steam density, in kg/m^3 ; r_{LV} is the latent heat of vaporization, in kJ/kg ; ν_L is the liquid kinematic viscosity, in m^2/s ; λ_L is the fluid thermal conductivity, in $W/(m \cdot ^\circ C)$; T_{sat} is the steam saturation temperature, in $^\circ C$ and T_P is the mean wall temperature, in $^\circ C$.

Subsequently, [17], the simultaneous solution of the differential equations of energy, momentum, continuity and conductivity was demonstrated, using the function of Tjonov (infinite line) as a weak substitute variable and linear discretization of a finite element one-dimensional three nodes. The definitive solution is reduced to the use of two dimensionless groups, whose combination allows to determine the α_T coefficient for any orientation of the tubes. This element constitutes a scientific novelty, as no background of a similar method is found in the literature.

The analytical solution developed uses the dimensionless velocity criteria and the Crosser number. Through these two criteria, the intervals of applicability of the proposed methodology are established based on the orientation of the ducts, which was subsequently adjusted and correlated with 1192 experimental data reported by 20 researchers. The proposed model yields 11.8 percent of average deviation for horizontal tubes and 13.0 percent for inclined and vertical tubes. The formulation obtained is given and discussed [17]:

$$\text{Adimensional velocity } J_g = \frac{xG}{\sqrt{g d_i \rho_V (\rho_L - \rho_V)}} \quad (6)$$

$$\text{Crosser number } Z = \left(\frac{1-x}{x}\right)^{0.8} Pr_L^{0.4} \quad (7)$$

For vertical and inclined tubes

$$\text{Interval 1 } J_g \geq \frac{1}{2.37Z + 0.728} \quad (8)$$

$$\text{Interval 2 } 0.927e^{(-0.0868Z^{-1.165})} < J_g < \frac{1}{2.37Z + 0.728} \quad (9)$$

$$\text{Interval 3 } J_g \leq 0.927e^{(-0.0868Z^{-1.165})} \quad (10)$$

For horizontal tubes

$$\text{Interval 1 } J_g \leq 0.979(Z + 0.262)^{-0.618} \quad (11)$$

$$\text{Interval 1 } J_g > 0.979(Z + 0.262)^{-0.618} \quad (12)$$

In Eq. (6) to (12), Pr_L is the Prandtl number for single-phase; x is the thermodynamic vapor quality; G is the mass flux, in $\text{kg}/(\text{m}^2\text{s})$.

The proposed expression for the determination of the heat transfer coefficient by condensation inside horizontal tubes is given by Camaraza-Medina et al. [18]:

$$Nu_T = Nu_L \cdot \left\{ 4.9x^{0.9} \left[(1-x)^2 + \frac{(1-x)^{0.1}}{Pr^{0.37}} \right] \right\}^{0.8} \quad (13)$$

In Eq. (13) Pr is the reduced pressure. The mathematical deduction of the Eq. (13) and the elements associated are provided by Camaraza-Medina et al. [17].

For the determination of Nu_L , in the literature the use of Dittus-Boelter expression is a generalized criterion, however, recently the author showed that the correlation index could be improved by using a model derived from the Prandtl analogy, which is described as [19]:

$$Nu_L = \frac{(Re_L - 10^M) \cdot Pr_L}{A \cdot I^2 - J \cdot I \cdot (1 - Pr_L^{2/3})} \cdot \left(1 + \left(\frac{d_i}{l}\right)^{2/3} \right) \cdot \left(\frac{\mu_F}{\mu_P}\right)^{0.14} \quad (14)$$

where: Re_L is the liquid Reynolds number, μ_F is the Fluid dynamic viscosity at mean fluid temperature, in $a \cdot s$; μ_P is the fluid dynamic viscosity at wall temperature, in $Pa \cdot s$; l is the length of the tube, in m. The mathematical deduction of the Eq. (14) is given by Camaraza-Medina et al. [20], while the constants used are summarized in Table 4.

Table 4. Values of the constants used in Eq. (14)

	$2.3 \cdot 10^3 < Re < 1 \cdot 10^4$	$1 \cdot 10^4 \leq Re \leq 1 \cdot 10^4$
A	75.4	91.4
I	$\log(Re_L^{0.56}/3.196)$	
J	104	116.7
M	$-0.027[\log Re]^2 + 0.2 \log Re + 2.63$	
		0

Additional tests carried out allowed us to conclude that the combination of Eqns. (5) and (13) depending on the work zones, offers a better adjustment to the experimental values available for vertical and inclined tubes. This combination was developed is given by Camaraza-Medina et al. [18]:

$$\text{Interval 1 } Nu = Nu_{vert} \quad (15)$$

$$\text{Interval 2 } Nu = \sqrt{(Nu_T)^2 + (Nu_{vert})^2} \quad (16)$$

$$\text{Interval } Nu = Nu_{vert} \quad (17)$$

In Eq. (16), if $Re_V < 3.5 \cdot 10^4$, then $Nu_{vert} = 0$. Table 5 provides a detailed summary of parameters range that shows a satisfactory fit with Eqns. (15) to (17).

Table 5. Summary of the validity range for Eq. (15) to (17)

Parameter	Range
Fluids	Water, R-22, R-32, R-113, R-123, R-125, R-134a, R-142b, R-404a, R-410a, R-502, R-507, isobutene, propylene, propane, benzene, ethanol, methanol, toluene and dowerm 209.
d_i (mm)	2 - 50
G ($\text{kg}/\text{m}^2\text{s}$)	4 - 850
Pr_L	1 - 20
Z	0.005 - 20
Re_L	60 - 84830
Re_V	8210 - 523980
x	0.01 - 1
p_r	0.0008 - 0.91
Tube orientation	Horizontal, vertical and inclined
J_g	0.6 - 20

In Tables 6 and 7, the validity range of Eqns. (15) to (17) is fragmented into four intervals, while in Figures 3 and 4 the values of MAE and E_{max} obtained in the correlation developed between available experimental data and selected models are given in graphical form [15].

For vertical and inclined tubes only the Shah model is used for comparison, since the remaining ones are only valid for horizontal tubes. An analysis of Figures 3 and 4 shows that the Chato's formulation generates a low adjustment of average values, which are between 28 and 43 percent, with a maximum error rate close to 60 percent in the four zones.

For horizontal tubes, the Chato's Equation provides an MAE values in the range of 17 to 24 percent, with the best fit in zone 3, in which the values of p_r and d_i agree very well with the precepts under which the Chato model was developed.

In Tables 8 and 9, the validity range of the Eq. (14) is divided into six intervals. In Figures 5 and 6 the values of MAE and E_{max} obtained in the correlation developed between available experimental data and selected models are given in graphical form [15].

For transition zone $2.4 \times 10^3 \leq Re < 10^4$ (see Figure 5), the most unfavorable indicators are obtained using the models

of Dittus-Boelter and Mijeev, which provide MAE values respectively of 38.4% and 36.1% for 64.5% and 68.1% of the experimental data, respectively. Hausen's model allows to

obtain convenient results, with MAE values of 19.3% in 75.1% of the examined data, which agrees well with those results given by Su An and Kim [21].

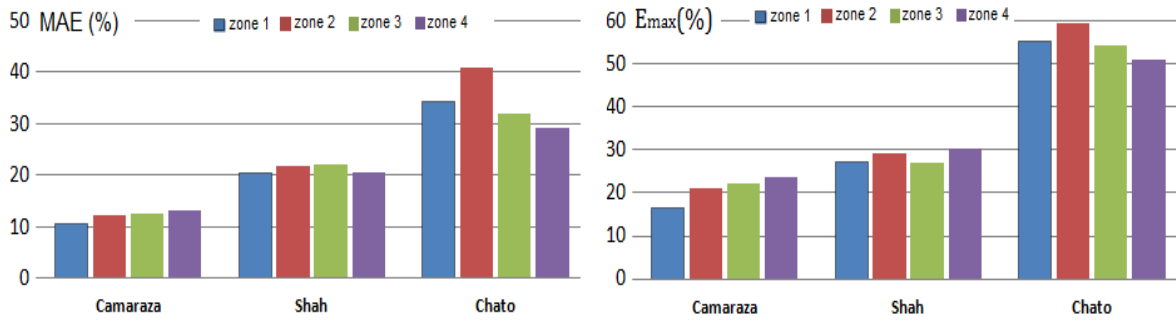


Figure 3. MAE and E_{max} values obtained in the correlation data with other models for vertical and inclined tubes

Table 6. Correlation of experimental values with respect to Eqns. (15) to (17)

Vertical and inclined tubes					
Zone	Validity range	Deviation	Zone	Validity range	Deviation
1	$Re_L \leq 9.8 \cdot 10^3$	$MAE < 10.6\%$ for 89.3% of the data	2	$Re_L \leq 59 \cdot 10^3$	$MAE < 12.2\%$ for 85.4% of the data
	$Re_v \leq 1.7 \cdot 10^5$			$Re_v \leq 3.33 \cdot 10^5$	
	$2 \leq d_i \leq 8.0$			$2 \leq d_i \leq 19.3$	
3	$38 \leq G \leq 300$	$E_{max} < 16.6\%$ $N = 148$	4	$3 \leq G \leq 468$	$E_{max} < 21.1\%$ $N = 479$
	$0.01 \leq x \leq 0.99$			$0.01 \leq x \leq 0.99$	
	$p_r \leq 0.1$			$p_r \leq 0.25$	
3	$Re_L \leq 59 \cdot 10^3$	$MAE < 12.4\%$ for 82.9% of the data	4	$Re_L \leq 59 \cdot 10^3$	$MAE < 13\%$ for 84.1% of the data
	$Re_v \leq 3.33 \cdot 10^5$			$Re_v \leq 3.33 \cdot 10^5$	
	$2 \leq d_i \leq 30$			$2 \leq d_i \leq 47.5$	
3	$3 \leq G \leq 538$	$E_{max} < 22.4\%$ $N = 542$	4	$3 \leq G \leq 598$	$E_{max} < 23.4\%$ $N = 584$
	$0.01 \leq x \leq 0.99$			$0.01 \leq x \leq 0.99$	
	$p_r \leq 0.44$			$p_r \leq 0.66$	

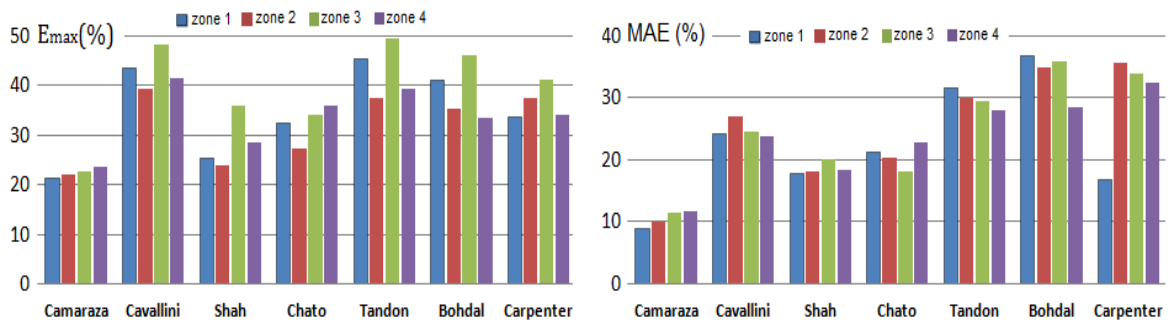


Figure 4. MAE and E_{max} values obtained in the correlation data with other models for horizontal tubes

Table 7. Correlation of experimental values with respect to Eqns. (15) to (17)

Horizontal tubes					
Zone	Validity range	Deviation	Zone	Validity range	Deviation
1	$Re_L \leq 6.4 \cdot 10^4$	$MAE < 8.9\%$ for 83.3% of the data	2	$Re_L \leq 7.0 \cdot 10^4$	$MAE < 10\%$ for 81.2% of the data
	$Re_v \leq 2.1 \cdot 10^5$			$Re_v \leq 4.8 \cdot 10^5$	
	$2 \leq d_i \leq 8.0$			$2 \leq d_i \leq 8.0$	
3	$38 \leq G \leq 300$	$E_{max} < 21.3\%$ $N = 265$	4	$38 \leq G \leq 600$	$E_{max} < 22.2\%$ $N = 436$
	$0.01 \leq x \leq 0.99$			$0.01 \leq x \leq 0.99$	
	$p_r \leq 0.1$			$p_r \leq 0.3$	
3	$Re_L \leq 8.5 \cdot 10^4$	$MAE < 11.5\%$ for 81.9% of the data	4	$Re_L \leq 8.5 \cdot 10^4$	$MAE < 11.8\%$ for 84.3% of the data
	$Re_v \leq 5.9 \cdot 10^5$			$Re_v \leq 6 \cdot 10^5$	
	$2 \leq d_i \leq 18.9$			$2 \leq d_i \leq 49$	
3	$38 \leq G \leq 750$	$E_{max} < 22.7\%$ $N = 538$	4	$38 \leq G \leq 850$	$E_{max} < 23.6\%$ $N = 608$
	$0.01 \leq x \leq 0.99$			$0.01 \leq x \leq 0.99$	
	$p_r \leq 0.5$			$p_r \leq 0.91$	

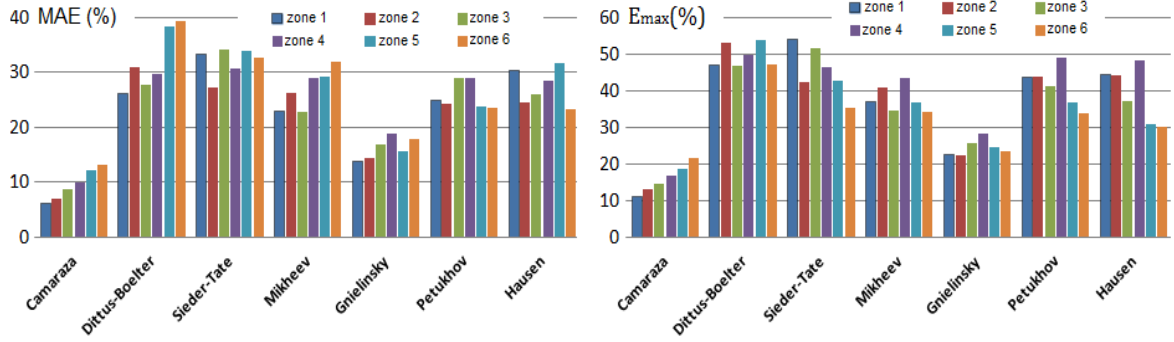


Figure 5. MAE and E_{max} values obtained in the correlation data with other models for $2.4 \cdot 10^3 \leq Re < 10^4$

Table 8. Correlation of the first range of values with Eq. (14)

Valid to $2.4 \cdot 10^3 \leq Re_L < 10^4$ (transient flow)					
Zone	Validity range	Deviation	Zone	Validity range	Deviation
1	$Pr_L \leq 10^2$ $\mu_F/\mu_P \leq 12.4$	$EMA < 6.1\%$ for	2	$Pr_L \leq 2 \cdot 10^2$ $\mu_F/\mu_P \leq 18.4$	$EMA < 7\%$ for
		91.3% of the data			90.4% of the data
3	$Pr_L \leq 2 \cdot 10^3$ $\mu_F/\mu_P \leq 22.2$	$E_{max} < 11.2\%$	4	$Pr_L \leq 8.1 \cdot 10^3$ $\mu_F/\mu_P \leq 34.2$	$E_{max} < 13.1\%$
		$N = 209$			$N = 387$
5	$Pr_L \leq 1.2 \cdot 10^4$ $\mu_F/\mu_P \leq 62.2$	$EMA < 8.7\%$ for	6	$Pr_L \leq 4.7 \cdot 10^4$ $\mu_F/\mu_P \leq 177$	$EMA < 10\%$ for
		89.1% of the data			88.2% of the data
		$E_{max} < 14.7\%$			$E_{max} < 16.8\%$
		$N = 506$			$N = 617$
		$EMA < 10.7\%$ for			$EMA < 13.6\%$ for
		86.4% of the data			80.4% of the data
		$E_{max} < 18.9\%$			$E_{max} < 21.8\%$
		$N = 789$			$N = 1003$

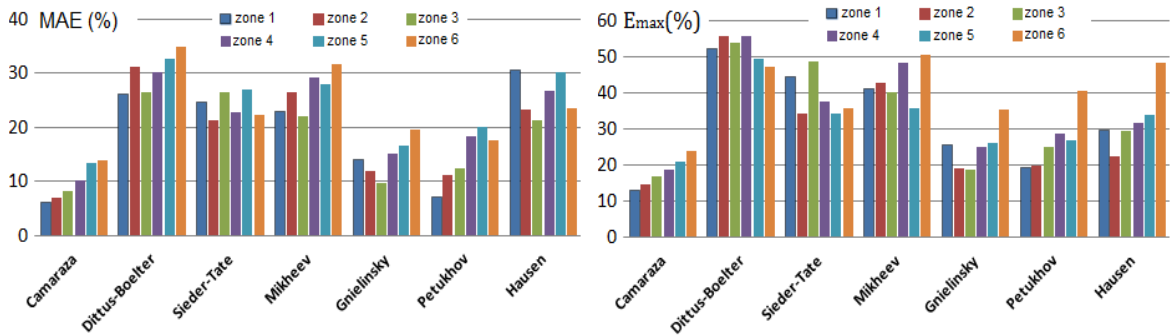


Figure 6. MAE and E_{max} values obtained in the correlation data with other models for $10^4 < Re \leq 8.2 \cdot 10^6$

Table 9. Correlation of the second range of values with Eq. (14)

Valid to $10^4 < Re_L \leq 8.2 \cdot 10^6$ (Turbulent flow)					
Zone	Validity range	Deviation	Zone	Validity range	Deviation
1	$Pr_L \leq 10^2$ $\mu_F/\mu_P \leq 12.4$	$EMA < 13.1\%$ for	2	$Pr_L \leq 2 \cdot 10^2$ $\mu_F/\mu_P \leq 18.4$	$EMA < 14.8\%$ for
		89.4% of the data			88.3% of the data
3	$Pr_L \leq 2 \cdot 10^3$ $\mu_F/\mu_P \leq 22.2$	$E_{max} < 12.8\%$	4	$Pr_L \leq 8.1 \cdot 10^3$ $\mu_F/\mu_P \leq 34.2$	$E_{max} < 14.1\%$
		$N = 419$			$N = 795$
5	$Pr_L \leq 1.2 \cdot 10^4$ $\mu_F/\mu_P \leq 62.2$	$EMA < 8.3\%$ for	6	$Pr_L \leq 4.7 \cdot 10^4$ $\mu_F/\mu_P \leq 177$	$EMA < 10.2\%$ for
		86.1% of the data			85.3% of the data
		$E_{max} < 16.9\%$			$E_{max} < 18.7\%$
		$N = 1127$			$N = 1414$
		$EMA < 11.3\%$ for			$EMA < 14\%$ for
		83.1% of the data			80.8% of the data
		$E_{max} < 20.9\%$			$E_{max} < 24.1\%$
		$N = 1715$			$N = 2093$

The correlations of Petukhov and Sieder-Tate are not valid in this interval; however, they provide an adequate result, with MAE values of 24.6 and 29.4% for 72.4 and 70.5% of the experimental data, respectively; this indicates that they can be

used for rapid estimations of the heat transfer coefficients in the transition zone, which confirms the recommendations given by Su An and Kim [21].

For turbulent zone $10^4 \leq Re < 8.2 \times 10^6$ (see Figure 6),

the most unfavorable indicators are obtained with the Dittus-Boelter and Sieder-Tate models. The first provides *MAE* values of 21.6% and 39.3% for 74.2% and 66.7% of the data, for Zones 1 and 6, respectively. The second model shows *MAE* values of 14.3% and 36.5% for 80.9% and 72.4% of the experimental data, for Zones 1 and 6, respectively.

The models by Mijeev and Hausen allow obtaining convenient correlation results. Hausen's model provides *MAE* values of 9.8% and 20.4% for 85.2% and 74.2% of the experimental data, for Zones 1 and 6, respectively. The model by Mijeev shows *MAE* values of 15.5% and 32.8% for 77.6% and 70.2% of the experimental data, for Zones 1 and 6, respectively.

4. CONCLUSIONS

The correlation and adjustment of available experimental data facilitated the development of new models that allow reducing the uncertainty in the determination of the internal and external film coefficients, being established a comparison between the proposal and other existing relationships in the literature, which results in a lower dispersion margin for the models described in this work.

The average correlation error in the determination of the α_L and α_T coefficients is reduced for external and internal flow up to 6.9 and 13 percent respectively. Regarding the elements of study presented, there is no evidence of similar expressions in the available and known literature, which is why they are considered a scientific novelty.

ACKNOWLEDGMENT

The author is very grateful for the help provided by Professor S. Thomson, from the Department of Mathematics, Massachusetts Institute of Technology, USA and Dr. Moustafa Zeki Yilmazoglu, from the Department of Mechanical Engineering, Gazi University, Turkey.

REFERENCES

- [1] Huang, X., Chen, L., Kong, Y., Yang, L., Du, X. (2018). Effects of geometric structures of air deflectors on thermo-flow performances of air-cooled condenser. *International Journal of heat and Mass Transfer*, 118: 1020-1032. <https://doi.org/10.1016/j.ijheatmasstransfer.2017.11.071>
- [2] ECI AZ. (2019). Datos técnicos e ingeniería básica para el proyecto de instalación de centrales eléctricas de biomasa en el quinquenio 2020-2025, (ECIAZ, SA.), La Habana.
- [3] INRH. (2020). Boletín de Análisis de lluvias, embalses, acuíferos y costo del agua, Dirección de Uso Racional del Agua, INRH, La Habana. <http://www.inrh.gob.cu/03-2020.htm>, accessed on May 17, 2020.
- [4] IDEA. (2020). World Energy Resources 2020, Oklahoma University State, 21-23.
- [5] Owen, M., Kröger, D.V. (2017). A numerical investigation of vapor flow in large air-cooled condensers. *Applied Thermal Engineering*, 127: 157-164. <http://dx.doi.org/10.1016/j.applthermaleng.2017.08.026>
- [6] Deng, H., Liu, J., Zheng, W. (2019). Analysis and comparison on condensation performance of core tubes in air-cooling condenser. *International Journal of Heat and Mass Transfer*, 135: 717-731. <https://doi.org/10.1016/j.ijheatmasstransfer.2019.02.011>
- [7] Yuan, W., Sun, F., Zhao, Y., Chen, X., Li, Y., Lyu, X. (2020). Numerical study on the influence mechanism of crosswind on frozen phenomena in a direct air-cooled system. *Energies*, 13: 3831. <https://doi.org/10.3390/en13153831>
- [8] Li, J., Bai, Y., Li, B. (2018). Operation of air cooled condensers for optimized back pressure at ambient wind. *Applied Thermal Engineering*, 128: 1340-1350. <https://doi.org/10.1016/j.applthermaleng.2017.09.122>
- [9] Deng, H., Liu, J. (2019). Performance prediction of finned air-cooled condenser using a conjugate heat-transfer model. *Applied Thermal Engineering*, 150: 386-397. <https://doi.org/10.1016/j.applthermaleng.2019.01.012>
- [10] Jin, R., Yang, X., Yang, L., Du, X., Yang, Y. (2018). Square array of air-cooled condensers to improve thermo-flow performances under windy conditions. *International Journal of heat and Mass Transfer*, 127: 717-729. <https://doi.org/10.1016/j.ijheatmasstransfer.2018.06.135>
- [11] Loganathan, P., Dhivya, M. (2018). Thermal and mass diffusive studies on a moving cylinder entrenched in a porous medium. *Latin American Applied Research*, 48(2): 119-124.
- [12] Gama, R.M.S. (2019). Non-linear problem arising from the description of the wave propagation in linear elastic rods. *Latin American Applied Research*, 49(1): 61-63.
- [13] Cano-Moreno, J.D., Cabanellas-Becerra, J.M. (2019). Experimental validation of an escalator simulation model. *Latin American Applied Research*, 49(3): 187-192.
- [14] Camaraza-Medina, Y., Rubio-Gonzales, A.M., Cruz-Fonticiella, O.M., Garcia-Morales, O.F., Vizcon-Toledo, R., Quiza-Sardiñas, R. (2018). Simplified analysis of heat transfer through a finned tube bundle in air-cooled-condenser-second assessment. *Mathematical Modelling of Engineering Problems*, 5(4): 365-372. <http://doi.org/10.18280/mmep.050413>
- [15] Camaraza, Y. (2017). Introducción a la termodinámica. Editorial Universitaria, La Habana.
- [16] Medina, Y.C., Khandy, N.H., Carlson, K.M., Fonticiella, O.M.C., Morales, O.F.C. (2018). Mathematical modeling of two-phase media heat transfer coefficient in air-cooled condenser systems. *International Journal of Heat and Technology*, 36(1): 319-324. <https://doi.org/10.18280/ijht.360142>
- [17] Camaraza-Medina, Y., Hernandez-Guerrero, A., Luviano-Ortiz, J.L., Cruz-Fonticiella, O.M., García-Morales, O.F. (2019). Mathematical deduction of a new model for calculation of heat transfer by condensation inside pipes. *International Journal of Heat and Mass Transfer*, 141: 180-190. <https://doi.org/10.1016/j.ijheatmasstransfer.2019.06.076>
- [18] Camaraza-Medina, Y., Hernández-Guerrero, A., Luviano-Ortiz, J.L., Mortensen-Carlson, K., Cruz-Fonticiella, O.M., García-Morales, O.F. (2019). New model for heat transfer calculation during film condensation inside pipes. *International Journal of Heat and Mass Transfer*, 128: 344-353. <https://doi.org/10.1016/j.ijheatmasstransfer.2018.09.012>
- [19] Camaraza-Medina, Y., Cruz-Fonticiella, O.M., García-

- Morales, O.F. (2019). New model for heat transfer calculation during fluid flow in single phase inside pipes. *Thermal Science and Engineering Progress*, 11: 162-166. <https://doi.org/10.1016/j.tsep.2019.03.014>
- [20] Camaraza-Medina, Y., Mortensen-Carlson, K., Guha, P., Rubio-Gonzales, A.M., Cruz-Fonticiela O.M., García-Morales, O.F. (2019). Suggested model for heat transfer calculation during fluid flow in single phase inside pipes (II). *International Journal of Heat and Technology*, 37(1): 257-266. <https://doi.org/10.18280/ijht.370131>
- [21] An, C.S., Kim, M.H. (2018). Thermo-hydraulic analysis of multi-row cross-flow heat exchangers. *International Journal of Heat and Mass Transfer*, 120: 534-539. <https://doi.org/10.1016/j.ijheatmasstransfer.2017.12.088>